Supporting Information

Hierarchically Structured Superhydrophobic Composite Films for Efficient Radiative Cooling and Energy Saving

Ruiming Tan[a], Hongbin Zhang[a], Le Wang[a], Yinyan Li[a], Peng Xue[b]*, Shiqing Xu[a], Gongxun Bai[b]*

[a] Key Laboratory of Rare Earth Optoelectronic Materials and Devices of Zhejiang Province, China Jiliang University, Hangzhou 310018, China.

[b] Beijing Key Laboratory of Green Building Environment and Energy Saving Technology, Beijing University of Technology, Beijing 100124, China.

E-mail address: xp@bjut.edu.cn (P. Xue), baigx@cjlu.edu.cn (G. Bai)

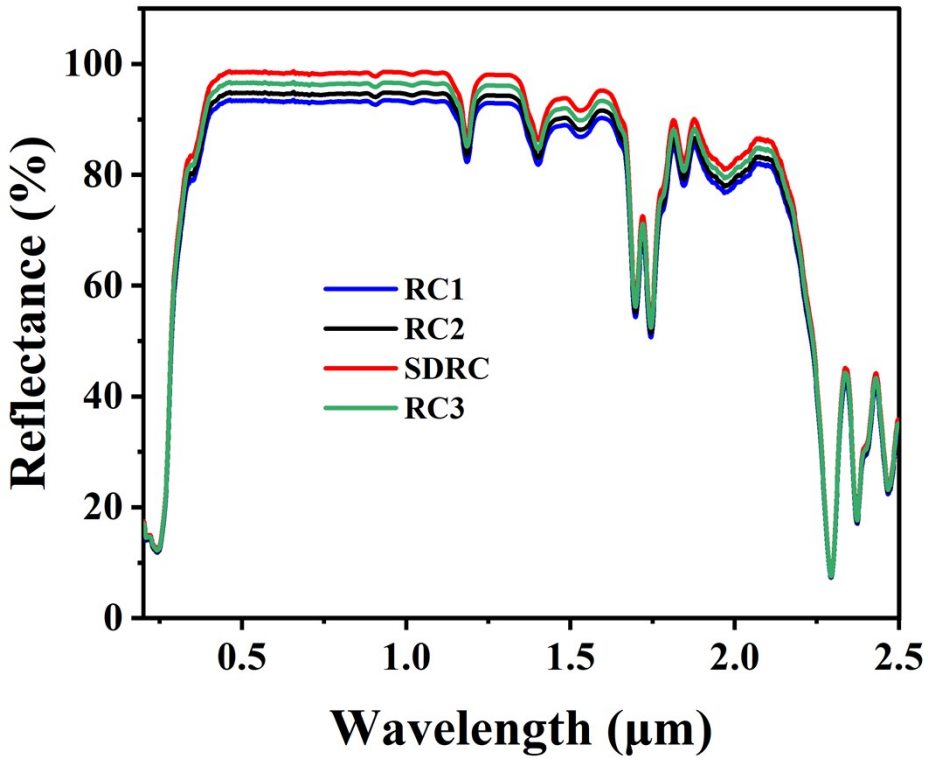

Fig. S1. The reflection spectra of the different samples were analyzed to compare their optical properties.

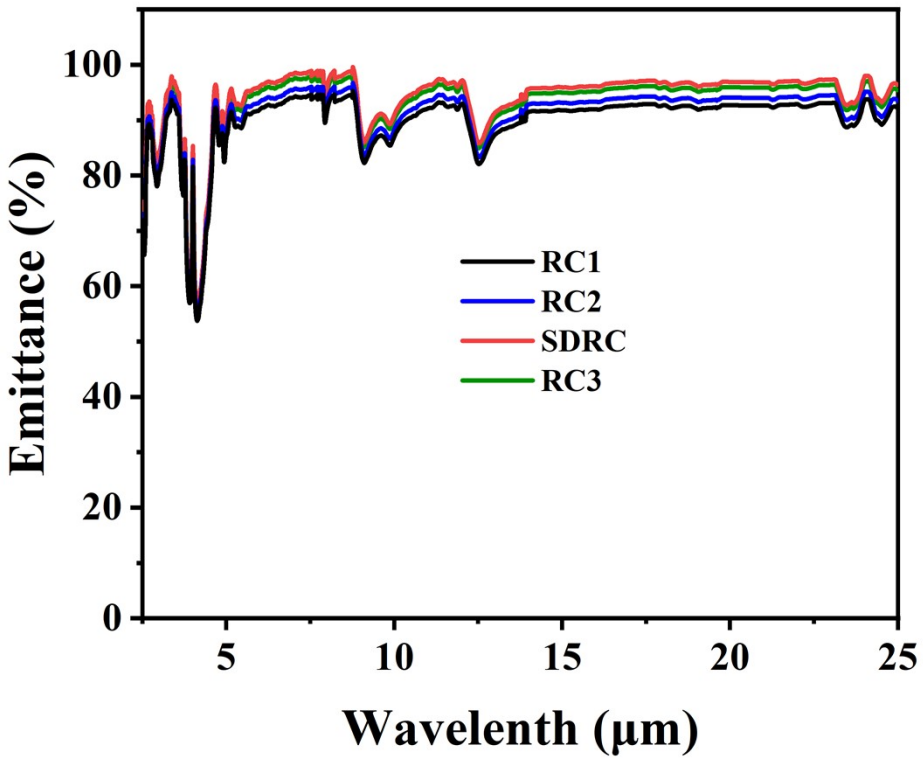

Fig. S2. The emission spectra of the different samples were analyzed to compare their optical properties.

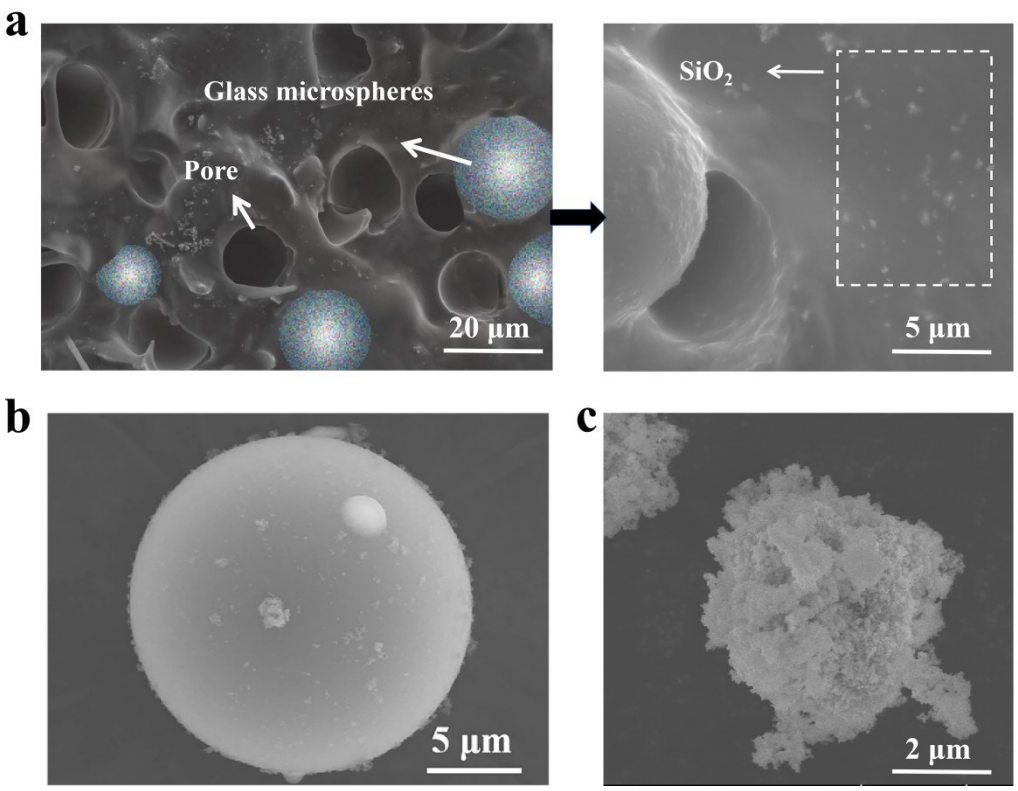

Fig. S3. (a) SEM image of the surface of the fabricated SDRC film, with the right image showing a magnified view. The glass microspheres and SiO_2 are well embedded in the PDMS matrix. (b) SEM morphology of the micron-sized glass microspheres. (c) SEM morphology of the nanoscale SiO_2 powders.

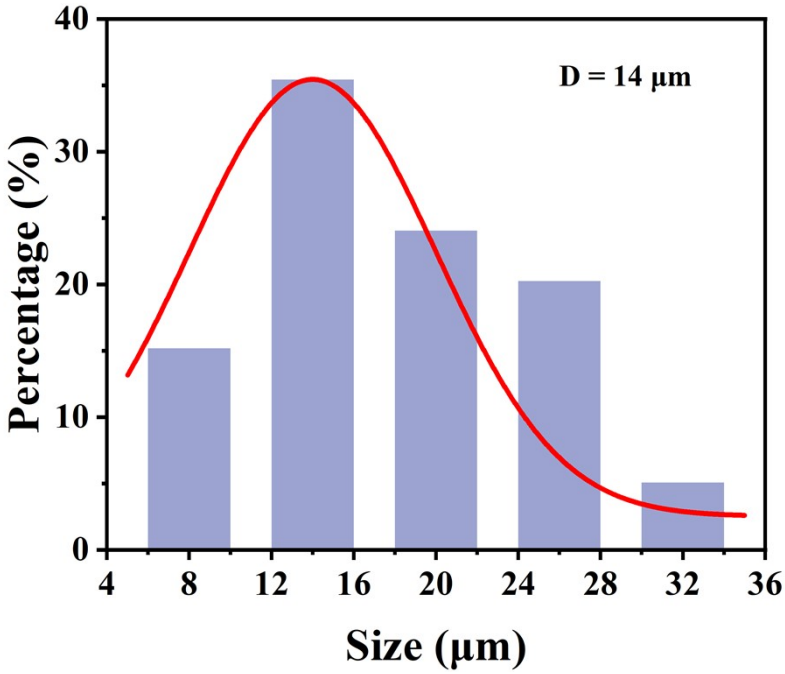

Fig. S4. Particle size distribution of glass microspheres.

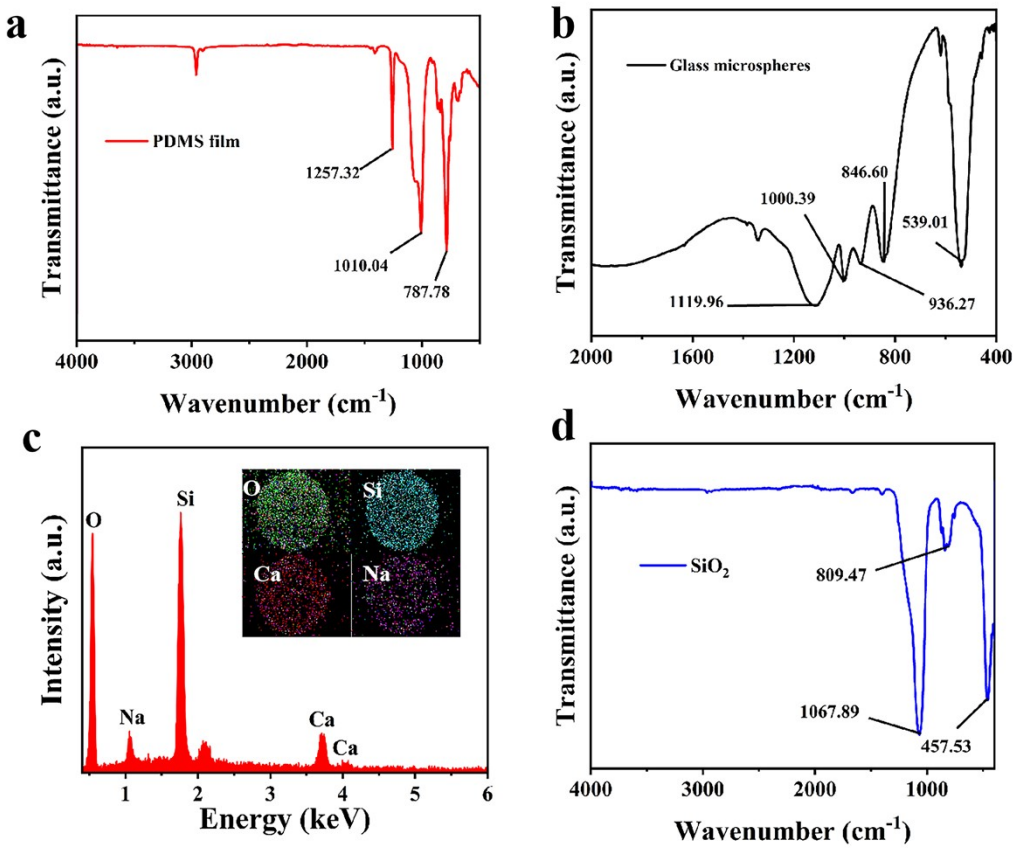

Fig. S5. (a) FTIR spectrum of PDMS fillm. (b) FTIR spectrum of glass microspheres. (c) The EDS energy spectrum of glass microspheres, with the elemental mapping of O, Si, Ca, and Na interpolated within the image. (d) FTIR spectrum of SiO_2 powders.

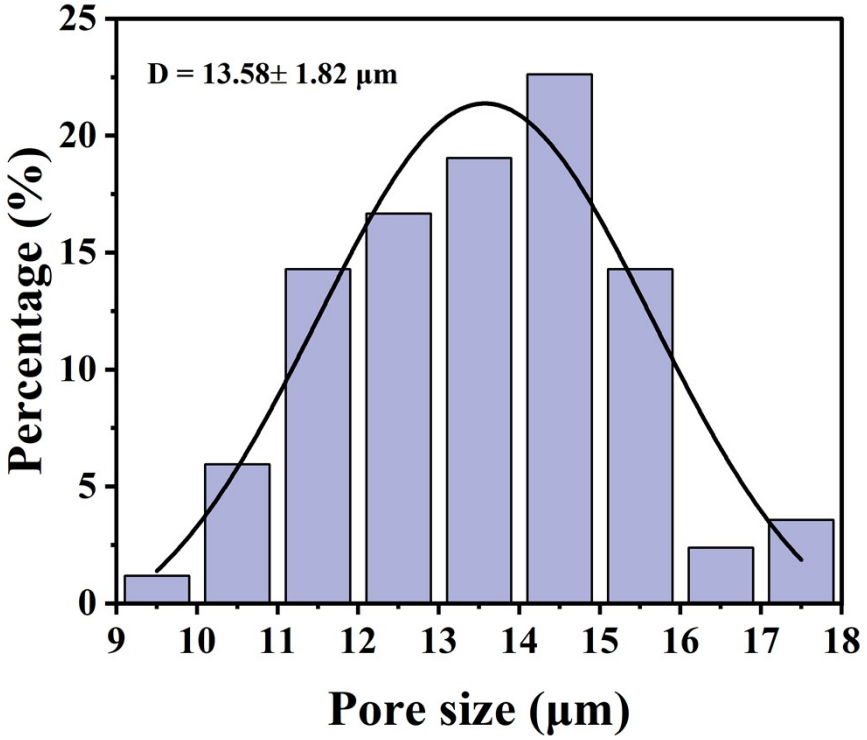

Fig. S6. Pore size distribution analysis of the SDRC film surface.

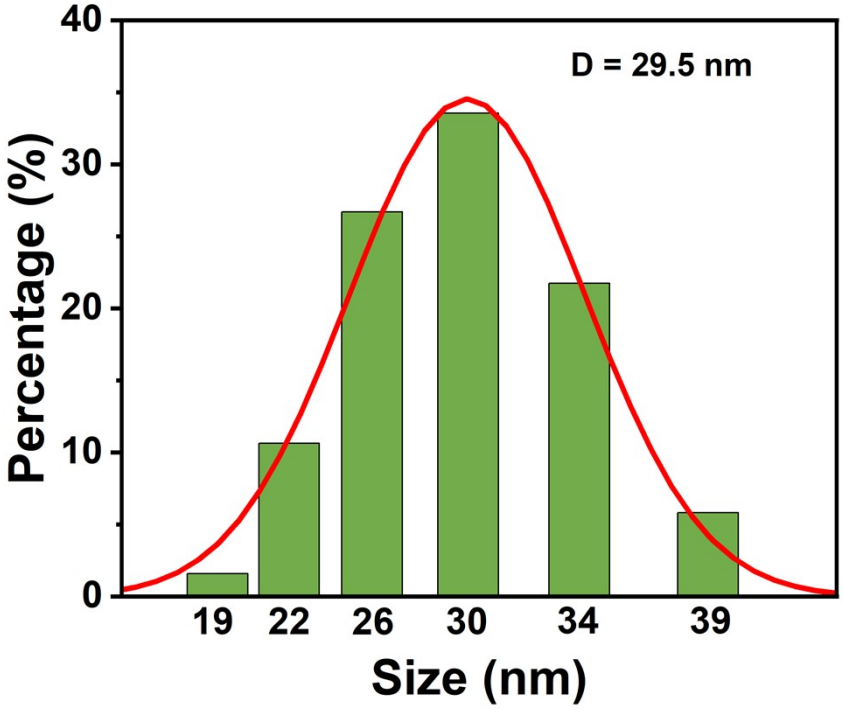

Fig. S7. Particle size analysis of nanoscale SiO_2.

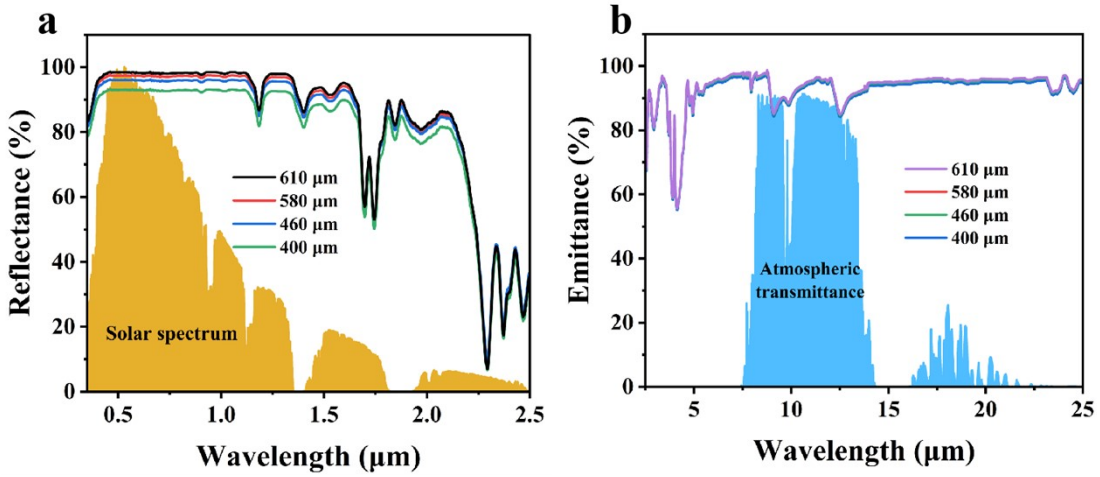

Fig. S8. (a) Reflectance spectra of SDRC films with varying thicknesses.

(b) Emissivity spectra of SDRC films with varying thicknesses.

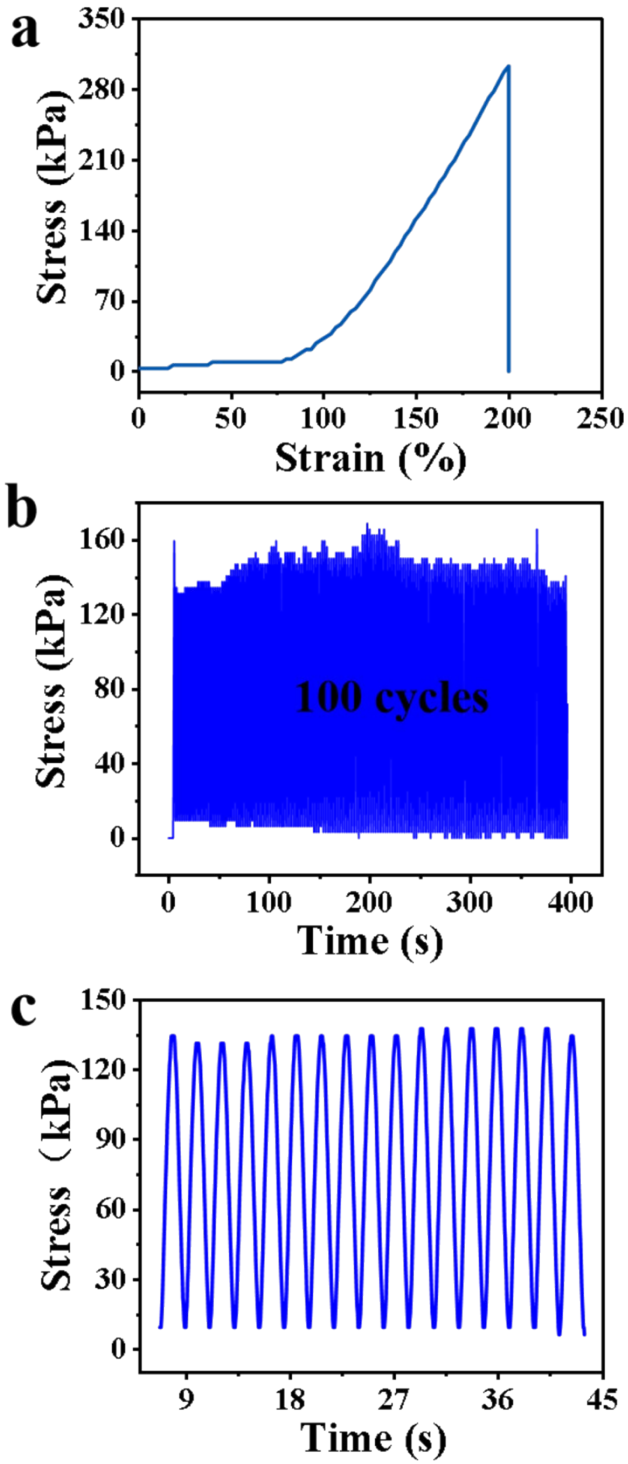

Fig. S9. (a) The stress-strain curve of SDRC film. (b) The stress-strain image after 100 cycles. (c) Mechanical properties testing of thin films.

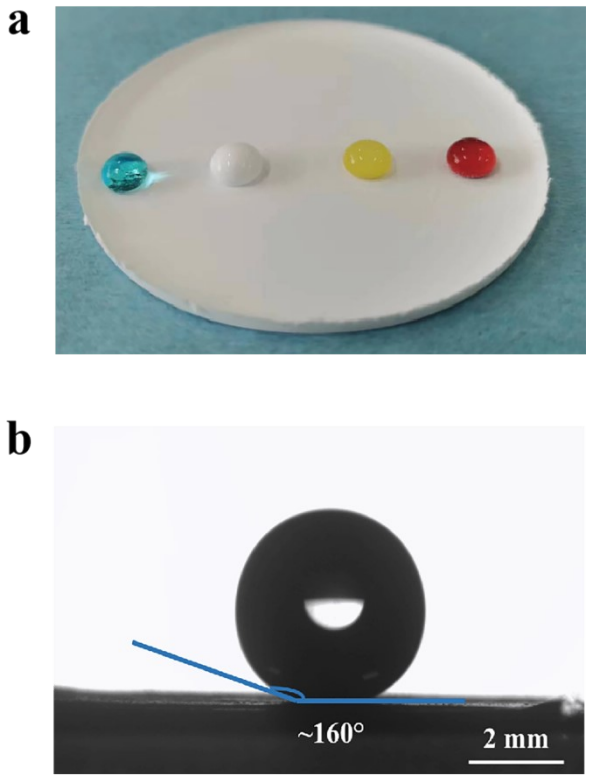

Fig. S10. (a) The Photographs of colored spherical water droplets on SDRC films. (b) The water contact angle image of SDRC film.

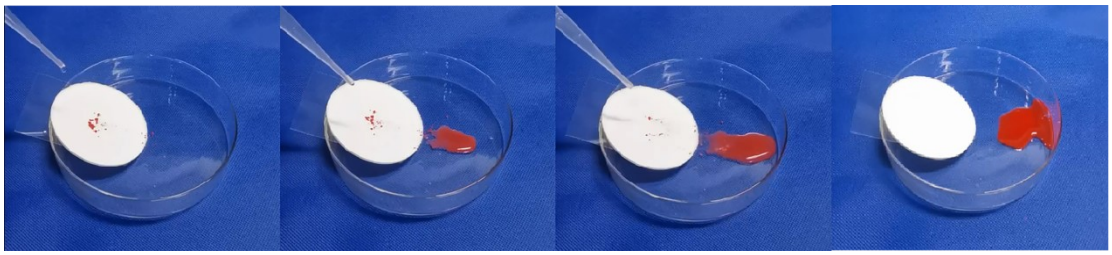

Fig. S11. The dyestuff removal process of the SDRC film rinsed by water droplet.

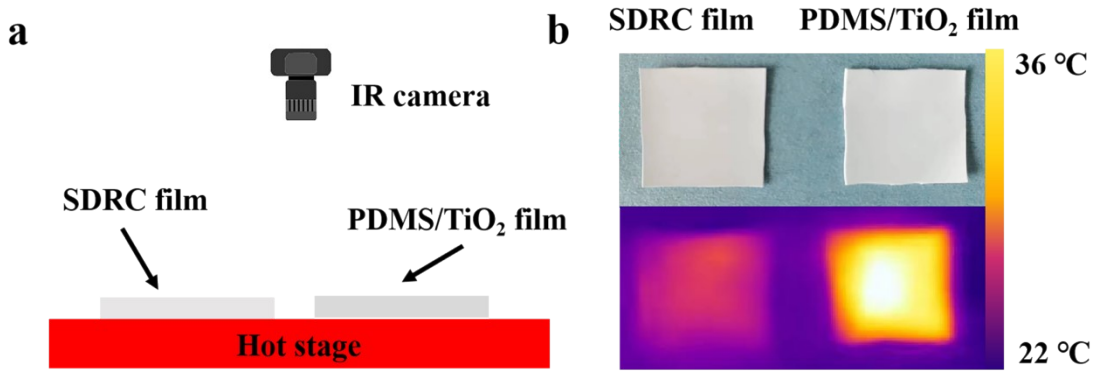

Fig. S12. (a) Schematic of the experiment examining the surface temperatures of samples on a hot stage. (b) Optical photographs and thermal images of the SDRC film (left) and PDMS/TiO_2 film (right) on the same hot stage.

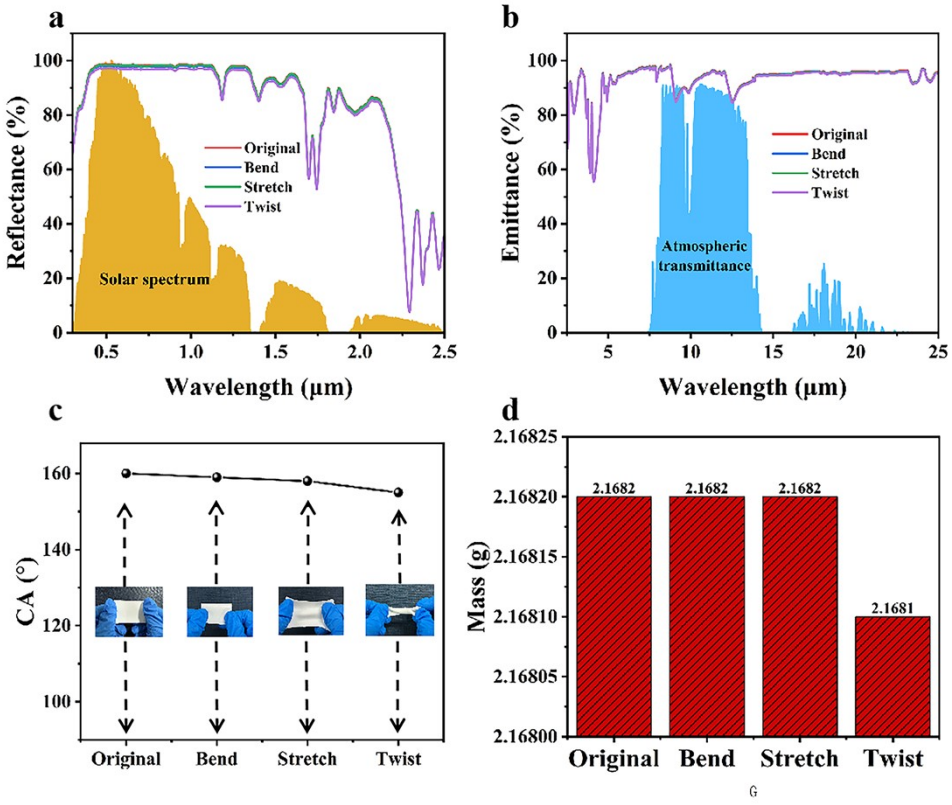

Fig. S13. (a) Reflectance measurements of the SDRC film after bending, stretching, and twisting. (b) Emissivity measurements of the SDRC film after bending, stretching, and twisting. (c) Water contact angle measurements of the SDRC film after bending, stretching, and twisting. (d) Mass measurements of the SDRC film after bending, stretching, and twisting.

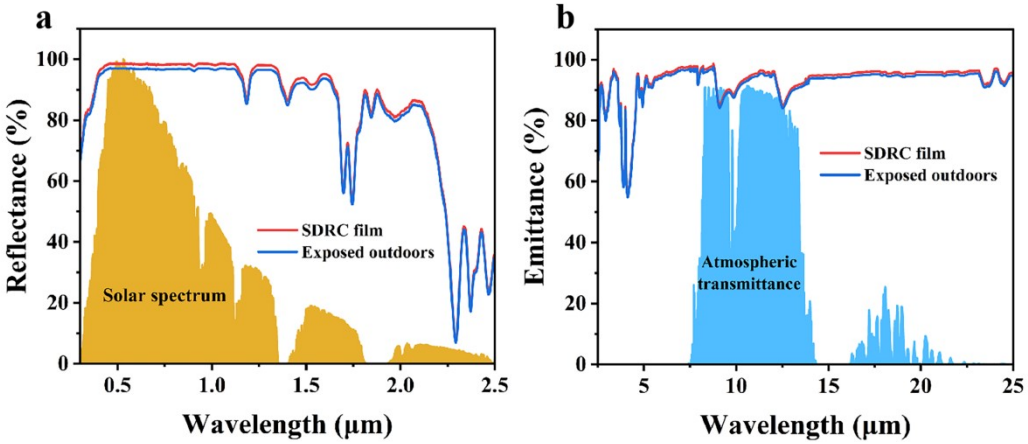

Fig. S14. (a) Reflectance spectra of the SDRC film measured after 10-day outdoor exposure followed by 3-month sealed storage. (b) Emissivity spectra of the SDRC film measured after 10-day outdoor exposure followed by 3-month sealed storage.

Table S1. The mass ratios of PDMS, glass microspheres and SiO_2 in the composite film.

Samples	PDMS (%)	Glass microspheres (%)	SiO_2 (%)
RC1	70	0	30
RC2	70	20	10
SDRC	**70**	**25**	**5**
RC3	70	30	0